Observing Turbulent Fragmentation in Simulations: Predictions for CARMA and ALMA

Mon. Not. R. Astron. Soc. **000**, 1–?? (2011) Printed 21 November 2011 (MN LATEX style file v2.2)

Observing Turbulent Fragmentation in Simulations: Predictions for CARMA and ALMA

Stella S. R. Offner,[1⋆] John Capodilupo,[2] Scott Schnee[3] and Alyssa A. Goodman[1]
[1] *Harvard-Smithsonian Center for Astrophysics, Cambridge, MA 02138*
[2] *Harvard University, Cambridge, MA 02138*
[3] *NRAO, Charlottesville, VA 22903*

21 November 2011

ABSTRACT

Determining the initial stellar multiplicity is a challenging problem since protostars are faint and deeply embedded at early times; once formed, multiple protostellar systems may significantly dynamically evolve before they are optically revealed. Interferometers such as CARMA and ALMA make it possible to probe the scales at which turbulent fragmentation occurs in dust continuum emission, potentially constraining early stellar multiplicity. In this Letter we present synthetic observations of starless and protostellar cores undergoing fragmentation on scales of a few thousand AU to produce wide binary systems. We show that interferometric observations of starless cores by CARMA should be predominantly featureless at early stages, although wide protostellar companions should be apparent. The enhanced capabilities of ALMA improve the detection of core morphology so that it may be possible to detect substructure at earlier times. In either case, spatial filtering from interferometry reduces the observed core substructure and often eradicates traces of existing filamentary morphology on scales down to 0.025 pc. However, some missing structure may be recaptured by combining data from the ALMA full science and Atacama compact arrays.

Key words: stars: formation, stars: starless cores, stars:low-mass

1 INTRODUCTION

While the initial mass function of stars is well measured, the initial stellar multiplicity remains largely unconstrained (Duchêne et al. 2007). Determining multiplicity among field stars well after the formation process has ended is itself a challenging problem: close binaries are often unresolvable, gravitational boundedness is difficult to confirm, and background stars are ever-present interlopers (Raghavan et al. 2010). During the formation and subsequent evolution, dynamical interactions influence initial companion separations and decrease multiplicity.

Observing the initial protostellar multiplicity in situ is challenging for similar reasons with the added complication that young protostars are dim and heavily obscured by dust and gas. However, recent interferometric instruments such as the Combined Array for Research in Millimeter-wave Astronomy (CARMA) and the Atacama Large Millimeter/submillimeter Array (ALMA) are revolutionizing the ability to probe the earliest stages of cores on scales of a few arcseconds or less. This presents an opportunity to observe core substructure, protostellar disks, and young companions.

There are two main theories of binary star formation. In the disk fragmentation scenario, massive protostellar accretion disks become Toomre unstable and fragment into one or more close companions (Adams et al. 1989; Bonnell & Bate 1994). In the turbulent fragmentation scenario, turbulent perturbations within a single prestellar core or filament individually collapse to form separate stars with wide separations (Goodwin et al. 2004; Fisher 2004; Goodwin et al. 2007). Numerical and analytic arguments indicate that disk instability should be quite common in high-mass star formation (Kratter & Matzner 2006; Kratter et al. 2008). However radiation feedback significantly reduces the fragmentation of disks around low-mass stars, resulting in few low-mass multiple star systems (Cai et al. 2008; Offner et al. 2009; Bate 2009). The multiple systems that do form are the result of turbulent fragmentation and have initial separations of ∼1000 AU (Offner et al. 2010).

The enhanced capabilities and sub-arcsecond resolution of ALMA will make it possible to test both scenarios of bi-

⋆ E-mail: soffner@cfa.harvard.edu

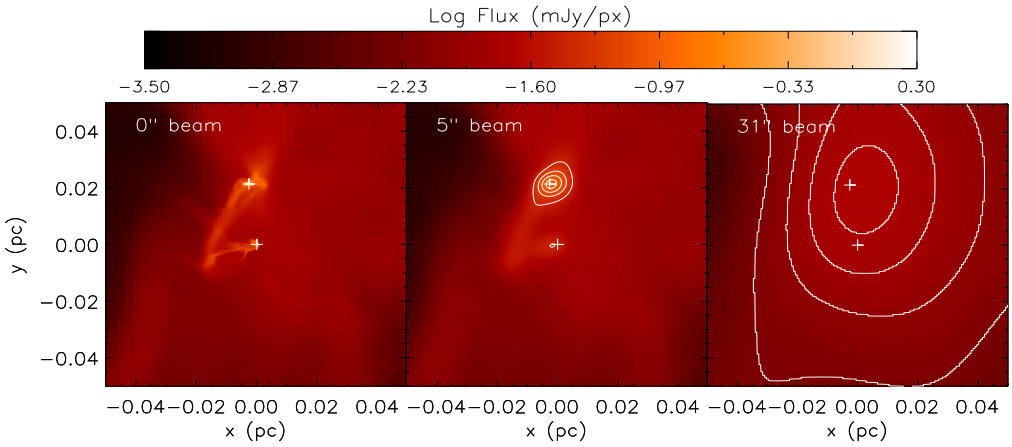

Figure 1. Single dish observation of 1.1 mm flux in mJy per pixel (0.13") of a binary protostellar system formed via turbulent fragmentation, where the system is placed at 250 pc. Left: Perfect resolution simulation data. Center: Image convolved with a 5" beam. Right: Image convolved with a 31" beam. The image extent is 80" across at a distance of 250 pc. Crosses mark the protostar positions. Contours indicate 30%, 50%, 70% and 90% of the image maximum.

nary formation and map protostellar accretion disks down to AU size scales. Several authors have used interferometric observations to look for young companions of Class 0 objects (e.g., Looney et al. 2000; Jørgensen et al. 2007; Maury et al. 2010). However, they arrive at somewhat different conclusions: Looney et al. (2000) find that all their targeted embedded objects have companions, while Maury et al. (2010) find only one tentative companion in a sample of five Class 0 sources. Likewise, Jørgensen et al. (2007) identified only one candidate previously unknown companion. Using continuum emission, it is possible in principle to detect companions forming as a result of turbulent fragmentation at even earlier times. For example, Schnee et al. (2010) use CARMA to observe 3mm continuum emission from 11 starless cores in the Perseus molecular cloud at 5" resolution. They found that the cores had no conspicuous substructure. This could be due to several possibilities. The cores may be too young or may never go on to form an individual star much less a wide multiple system. Turbulent fragmentation may be very uncommon. Or turbulent fragmentation may be ongoing in the cores, but beyond the observable limits of CARMA. We investigate the third possibility here.

If cores, such as those investigated by Schnee et al. (2010), actually contain young protostars, it might be possible to observe fragmentation at shorter wavelengths. Indeed, a number of very cold cores thought to be starless have since been found to contain protostars (Enoch et al. 2010; Dunham et al. 2011; Pineda et al. 2011). However, in the case of L1451, the presence of a protostar, potentially still in the "first core" gas stage, was ultimately identified by outflow activity rather than by thermal emission. This reinforces the point that source identification is challenging, and it requires instruments with high sensitivity and resolution to characterize core structure and identify young companions.

In this Letter, we use the CASA software package to synthetically observe binaries forming due to turbulent fragmentation in the numerical simulations of Offner et al. (2009). By following the evolution of such pairs beginning in the prestellar core stage, we can make predictions about the feasibility of observing such fragmentation in dust continuum and constraining stellar multiplicity at the earliest stage of star formation.

2 NUMERICAL SIMULATIONS AND METHODS

The molecular cloud simulations we observe in this letter are those presented in Offner et al. (2009). Since Offner et al. (2009) fully describe the calculations, we include only a brief overview here. The calculations are performed using the ORION adaptive mesh refinement code including driven large-scale turbulence, self-gravity, and flux-limited diffusion radiative transfer. Forming stars are modeled by sink particles with a sub-grid stellar evolution model. These are inserted in regions of the flow that exceed the maximum grid resolution. In practice, since protostellar winds are not included, these particles give an upper limit on the stellar mass. The cloud domain size is 0.65 pc across with a minimum cell size of 32 AU.

In our analysis, we focus on several typical systems out of the approximately 10 close pairs that form over the course of the simulation. Since the systems form self-consistently from the turbulent gas, the fragmentation history and stellar masses are not predetermined.

We use the "simdata" task in the Common Astronomy Software Applications (CASA) package[1] to produce synthetic interferometric observations of the starless and protostellar systems. Using simdata, the model cloud was placed at the RA and Dec of the Perseus molecular cloud. For the CASA input, we require maps of the cores in units of flux. Converting between simulated column density and continuum flux is straight-forward for optically thin emission. Assuming a constant dust temperature, T_D, the flux at a given frequency, ν, can related to the column density by:

[1] http://casa.nrao.edu

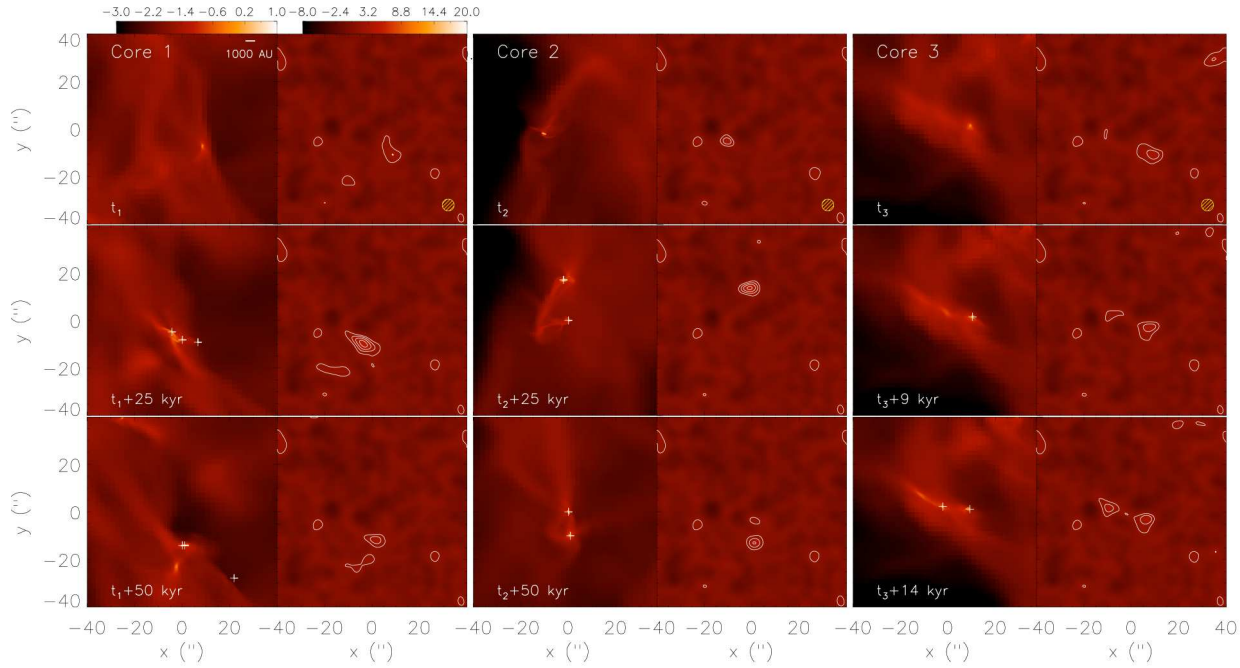

Figure 2. Comparison of simulations and CARMA synthetic observation for fragmenting cores at three different times. Left: Simulation data with perfect resolution in 1.1mm flux (Log mJy beam^{-1}). Color scale is the same as in Figure 1. Right: CARMA observation of each core at 3mm emission including Gaussian σ_S noise assuming a distance of 250 pc in mJy beam^{-1}. Contours indicate 30%, 50%, 70% and 90% of the maximum flux. The CARMA beamsize is indicated by the hatched ovals.

$$S_\nu = \Sigma B_\nu(T_D)\kappa_\lambda \Omega_b, \quad (1)$$

where $B_\nu(T_D)$ is the Planck function evaluated at the dust temperature, κ_λ is the dust opacity, Ω_b is the beam solid angle and Σ is the gas column density per pixel (e.g., Enoch et al. 2006). The opacities for 1.1 mm and 3 mm are $\kappa_{1.1} = 0.0114$ cm^2 g^{-1} and $\kappa_3 = 0.00169$ cm^2 g^{-1} (Ossenkopf & Henning 1994). The simulations assume that the dust and gas are well-coupled, which is a reasonable approximation for densities $> 10^4$ cm^{-3} (Goldsmith & Langer 1978). Thus, we adopt $T_D = 10$ K, the simulation gas temperature, which is also a lower limit for the dust temperature in Perseus (Schnee et al. 2009). Once protostars form, they heat their environment to mean temperatures of 15-20 K and result in higher emission.

Producing synthetic single dish observations of the simulations is a straight-forward application of equation 1. Finite resolution can then be imposed by convolving the flux map with a circular Gaussian beam.

3 SYNTHETIC OBSERVATIONS

For the purpose of comparison, we first present synthetic single dish observations of the fragmenting cores. We then produce interferometric observations mimicing the specifications of CARMA and ALMA. Finally, we investigate the influence of noise and distance on structure detection.

3.1 Single Dish Observations

Observations that map out entire molecular clouds and identify star-forming cores often use single dish continuum data. However, with beam resolutions of tens of arcseconds, resolving core substructure in even nearby clouds is impossible. Figure 1 shows a protostellar system forming in a dense core with 0" (i.e., perfect), 5" and 31" resolution. The two peaks are distinct with 5" resolution, although the fainter peak may not be apparent depending upon sensitivity and noise levels. At 31", a resolution comparable to SCUBA (850 μm) and Bolocam (1.1 mm), only a single peak is apparent.

Interferometers, such as CARMA, are able to achieve this 5" scale, but can only probe a fixed window of scales. Since larger scale information is resolved out, target fluxes may also be reduced by 90% or more relative to single dish observations. Figure 1 illustrates that cores forming wide protobinary companions *may* be observable with current interferometer technology.

3.2 CARMA Observations

We produce synthetic observations to compare with the CARMA observations of Schnee et al. (2010). In order to make a truly similar comparison, we reproduce their observing procedures and conditions as closely as possible. Our observations have a 2.8 GHz bandwidth centered at 102 GHz, and we adopt the CARMA D-array configuration and an integration time of 100 seconds with a total time of 8 hours. Unless otherwise stated, we assume the systems are 250 pc away: the distance of the Perseus molecular cloud. The pixel size of the simulated map is 0.13", and the synthesized beam is 5". We add synthetic Gaussian noise with $\sigma_S = 0.7$ mJy beam^{-1}, comparable to that of the Schnee et al. (2010) observations.

Figure 2 shows synthetic CARMA observations of three

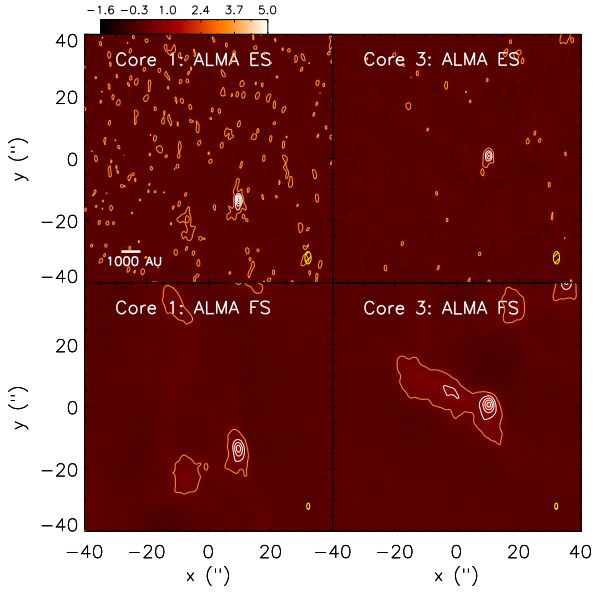

Figure 3. Comparison of early science (ES) and full science (FS) ALMA configurations for Core 1 (left) at t_1 and Core 3 (right) at t_3 assuming a distance of 250 pc. Color scale indicates flux in mJy beam^{-1}. The top two panels are observed with the early science (ES) extended configuration; the bottom two panels are observed in one example full science (FS) configuration. White contours indicate 30%, 50%, 70% and 90% of the maximum flux. Orange contours indicate 10% of the maximum flux. The ALMA beamsize is indicated by the hatched ovals.

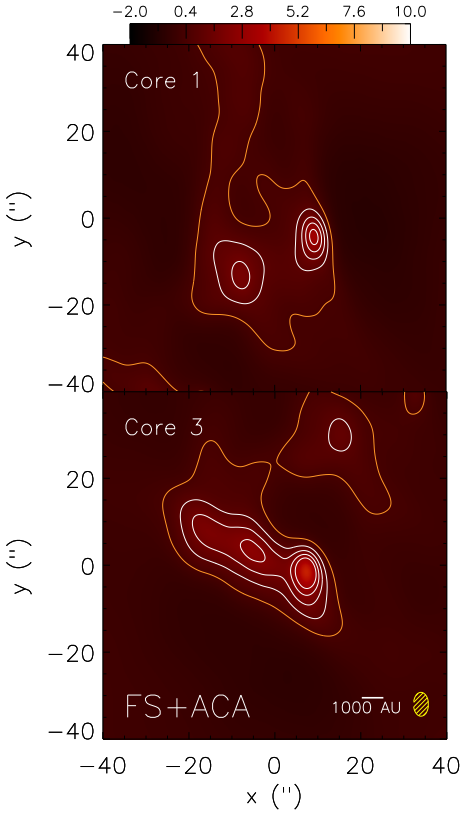

Figure 4. Synthetic observation combining data from ALMA FS with ALMA compact array for Core 1 (top) at t_1 and Core 3 (bottom) at t_3. Contours indicate fluxes with values 10% (orange), 30%, 50%, 70% and 90% of the maximum. The effective beamsize is indicated by the hatched oval. The observations assume 100s integration time and two hours of observing with each configuration.

separate cores undergoing turbulent fragmentation at three different times. The simulation data seen in 1.1 mm emission is plotted for comparison. At the first time all three cores are starless. However, each shows some evidence of collapse and fragmentation at perfect resolution. The second row illustrates that fragmentation proceeds on the order of 10-20 kyr, which is a relatively short time compared to the typical ∼100 kyr dynamical time of cores. If the core exists in a quasi-steady state for some time before undergoing collapse (e.g., Broderick et al. 2008), then the likelihood of catching any particular starless core in the act of fragmenting may be small. Such short timescales for observing close companions are consistent with those found by Stamatellos et al. (2011), who synthetically observed massive fragmenting disks. The probability is reduced further since not all cores (may) experience fragmentation on ∼ 1000 AU scales.

At the earliest times, interferometric observations do not clearly show fragmentation. The second fragment in Core 1 becomes more apparent over time, but is nearly invisible in the starless phase. However, the low level detections do appear similar in size and separation to some of the lower flux contours apparent in maps of Perbo45 and Perbo58 by Schnee et al. (2010). In contrast, all of the filamentary structure in the starless Cores 2 and 3 is resolved out. These results are consistent with the core observations of Schnee et al. (2010), who find that most starless cores that have bright 1.1mm emission in single dish maps are undetected in 3mm interferometric maps. This also confirms that additional filamentary structure may be removed by the interferometric technique.

The synthetic observations show that at later times the protostars and companions become brighter. Due to the factor of 10 difference in opacity, the over-densities will be significantly brighter in 1.1mm, which will increase the signal to noise. This suggests that widely separated protostellar companions should be relatively apparent at high resolution (e.g., Merrill & Enoch 2010). However, the length of the window in which fragmentation occurs is still problematic if secondaries migrate to shorter separations or are unbound on short timescales.

3.3 ALMA Predictions

ALMA, which will have 66 reconfigurable antennas, subarcsecond angular resolution and sensitivity to wavelengths from 3mm to 300 μm, will significantly expand observational capabilities. Although currently only partially completed, the ALMA early science program allows reduced observations with 16 12m operational antennas. Figure 3 shows simulated observations of Core 1 and Core 3 comparing the ALMA early science Cycle 0 extended configuration and the ALMA full science configuration 10. We adopt configuration 10 in the ALMA full science library in simdata since it is a representative intermediate configuration.

Each observation assumes a 100 second integration time and a total time of 2 hours. We add thermal noise to the

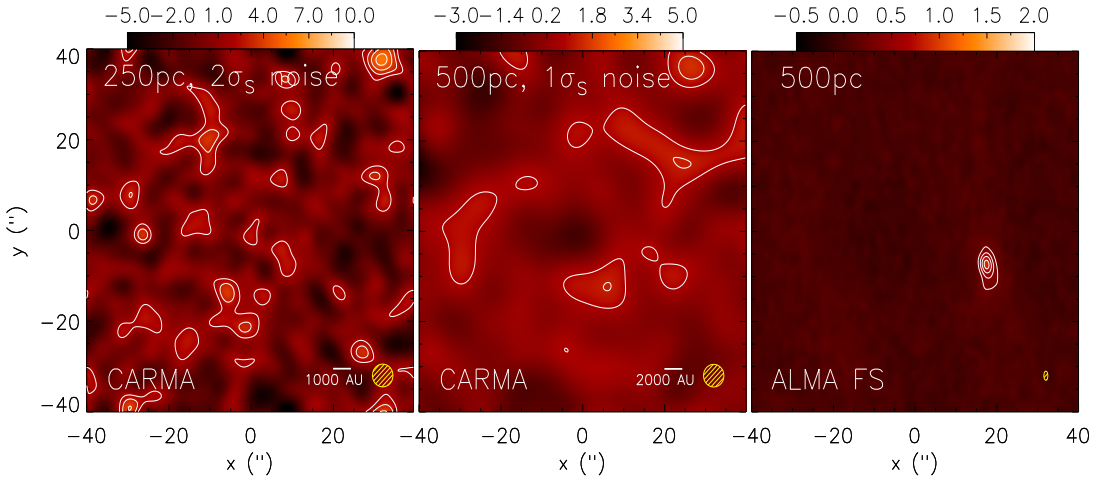

Figure 5. Left: Simulated 3mm CARMA observation of Core 1 at t_1 observed at a distance of 250 pc with $2\sigma_S$ noise. Center: Simulated 3mm CARMA observation of Core 1 observed at a distance of 500 pc with 1σ noise. Right: Simulated 3mm full science ALMA observation of Core 1 observed at a distance of 500 pc. Color scale shows flux in mJy beam^{-1}. Contours indicate fluxes with values 30%, 50%, 70% and 90% of the maximum. The beamsize is indicated by the hatched ovals.

simulated ALMA images using simdata, assuming that the precipitable water vapor (PWV) during the observations is 2.8mm (appropriate for Band 3 ALMA observations) and a bandwidth of 8 GHz. ALMA maps were cleaned until a threshold of 3 times the rms thermal noise in the map was reached. The pixel size, as for the CARMA simulations, is 0.13", and the early science and full science synthesized beam sizes are ∼3" and 1.5", respectively.

Figure 3 illustrates that ALMA better resolves the primary peak morphology. A secondary peak in Core 1 is marginally shown by contours with 10% of the maximum flux. However, the filamentary structure of Core 3 is not visible. The early science configuration sensitivity to substructure is otherwise similar to that of CARMA with four times the observing time. The ALMA full science configuration detects the Core 3 filament with some suggestion of further fragmentation. This highlights the difficulty of imaging structure and fragmentation even with ALMA's superior resolution.

It is possible to increase the range of recoverable spatial scales by combining data from antenna configurations with different baselines. The size of the ALMA 12-meter antennas prohibit them from being placed within 15 meters of one another, which limits the maximum resolvable spatial scale. To permit a greater range of observations, the completed ALMA site will include a second smaller array, the Atacama Compact Array (ACA), comprised of four 12-meter and 12 7-meter antennas. Here, we combine the higher spatial resolution synthetic data of the intermediate FS main array configuration with synthetic data from the 7-meter ACA antennas. Figure 4 shows a simulated observation of two cores where the visibilities from FS and ACA have been added and then deconvolved using the CASA CLEAN subroutine. The appearance of filamentary structure and core substructure is significantly improved compared to the single configuration data in Figures 2 and 3.

3.4 Noise and Resolution Limitations

Object distance and observation sensitivity are both critical to mapping core structure. Figure 5 shows Core 1 with increased noise and source distance. At our fiducial noise and resolution (see Figures 2 and 3) both increased noise and distance eliminate any detection with CARMA. At a distance of 500 pc, the secondary peak is also undetected with the ALMA full science configuration. However, the primary peak is reliably detected. This implies that fragmentation at later times, such as that illustrated in Core 1 at 50 kyr and Core 3 at $\geqslant$ 9 kyr, would be readily observable.

4 CONCLUSIONS

In this Letter we produce synthetic observations of fragmenting starless and protostellar cores. We show that interferometric observations of starless cores by CARMA should be predominantly featureless at early stages. In fact, structure may be apparent only within a short period, $\sim$ 10kyr, of the formation of a protostar. This may account for some of the apparent lack of substructure in starless cores noted by Schnee et al. (2010). We find that wide protostellar companions with separations of $\sim$ 1000AU should be detectable. The confidence of the secondary detection depends upon the source age, resolution, and signal-to-noise, which may partially explain the differing results of Looney et al. (2000), Jørgensen et al. (2007), and Maury et al. (2010). ALMA's enhanced capabilities improve the detection of core morphology, so that it may be possible to detect substructure at earlier times. Filamentary structure is more difficult to detect than peakiness, and interferometry, especially at high resolution, significantly reduces the presence and extent of filaments. However, we find that it is possible to recover missing structure by combining ALMA Full Science data with data from the Atacama Compact Array.

ACKNOWLEDGMENTS

This research has been supported by the NSF through grants AST-0901055 (SSRO) and AST-0908159 (AAG) and the Harvard College Program for Research in Science and Engineering (JC).

REFERENCES

Adams F. C., Ruden S. P., Shu F. H., 1989, *ApJ*, 347, 959
Bate M. R., 2009, *MNRAS*, 392, 1363
Bonnell I. A., Bate M. R., 1994, *MNRAS*, 269, L45
Broderick A. E., Narayan R., Keto E., Lada C. J., 2008, *ApJ*, 682, 1095
Cai K., Durisen R. H., Boley A. C., Pickett M. K., Mejía A. C., 2008, *ApJ*, 673, 1138
Duchêne G., Delgado-Donate E., Haisch Jr. K. E., Loinard L., Rodríguez L. F., 2007, Protostars and Planets V, pp 379–394
Dunham M. M., Chen X., Arce H. G., Bourke T. L., Schnee S., Enoch M. L., 2011, ArXiv e-prints
Enoch M. L., Lee J.-E., Harvey P., Dunham M. M., Schnee S., 2010, *ApJL*, 722, L33
Enoch M. L., Young K. E., Glenn J., Evans II N. J., Golwala S., Sargent A. I., Harvey P., Aguirre J., Goldin A., Haig D., Huard T. L., Lange A., Laurent G., Maloney P., Mauskopf P., Rossinot P., Sayers J., 2006, *ApJ*, 638, 293
Fisher R. T., 2004, *ApJ*, 600, 769
Goldsmith P. F., Langer W. D., 1978, *ApJ*, 222, 881
Goodwin S. P., Kroupa P., Goodman A., Burkert A., 2007, Protostars and Planets V, pp 133–147
Goodwin S. P., Whitworth A. P., Ward-Thompson D., 2004, *A&A*, 414, 633
Jørgensen J. K., Bourke T. L., Myers P. C., Di Francesco J., van Dishoeck E. F., Lee C.-F., Ohashi N., Schöier F. L., Takakuwa S., Wilner D. J., Zhang Q., 2007, *ApJ*, 659, 479
Kratter K. M., Matzner C. D., 2006, *MNRAS*, 373, 1563
Kratter K. M., Matzner C. D., Krumholz M. R., 2008, *ApJ*, 681, 375
Looney L. W., Mundy L. G., Welch W. J., 2000, *ApJ*, 529, 477
Maury A. J., André P., Hennebelle P., Motte F., Stamatellos D., Bate M., Belloche A., Duchêne G., Whitworth A., 2010, *A&A*, 512, A40+
Merrill M., Enoch M., 2010, in American Astronomical Society Meeting Abstracts #216 Vol. 41 of Bulletin of the American Astronomical Society, High Resolution VLA Observations of a Candidate Class 0 Binary Protostar. pp #422.07
Offner S. S. R., Klein R. I., McKee C. F., Krumholz M. R., 2009, *ApJ*, 703, 131
Offner S. S. R., Kratter K. M., Matzner C. D., Krumholz M. R., Klein R. I., 2010, *ApJ*, 725, 1485
Ossenkopf V., Henning T., 1994, *A&A*, 291, 943
Pineda J. E., Arce H. G., Schnee S., Goodman A. A., Bourke T., Foster J. B., Robitaille T., Tanner J., Kauffmann J., Tafalla M., Caselli P., Anglada G., 2011, ArXiv e-prints
Raghavan D., McAlister H. A., Henry T. J., Latham D. W., Marcy G. W., Mason B. D., Gies D. R., White R. J., ten Brummelaar T. A., 2010, *ApJ*s, 190, 1
Schnee S., Enoch M., Johnstone D., Culverhouse T., Leitch E., Marrone D. P., Sargent A., 2010, *ApJ*, 718, 306
Schnee S., Rosolowsky E., Foster J., Enoch M., Sargent A., 2009, *ApJ*, 691, 1754
Stamatellos D., Maury A., Whitworth A., André P., 2011, *MNRAS*, 413, 1787